Quantum Mechanical ab Initio Study of Mixed SiO_2-GeO_2 Crystals as Reference Models for Ge-Doped Silica Glasses

F. López-Gejo,*,‡ M. Busso,‡,† and C. Pisani‡,†

Unità INFM di Torino, Sezione F, Dipartimento di Chimica IFM, Università di Torino, via Giuria 5, I-10125 Torino, Italy

Received: September 6, 2002; In Final Form: February 5, 2003

In the present work, we have applied first principles quantum mechanical techniques to the study of periodic models of four silica polymorphs containing different proportions of germanium as a substitutional species: α-quartz, β-quartz, α-cristobalite, and stishovite (rutile); except for β-quartz, which is considered for the sake of completeness, these phases exist both in the pure silicon and pure germanium forms. Computations have been performed using both the Hartree−Fock (HF) approximation and the gradient corrected density functional PWGGA technique. A triple-ζ plus polarization basis set has been used. All geometries have been fully optimized at the HF level. Equilibrium structure, stability, and electronic properties of the mixed phases are analyzed with reference to the pure systems. It is shown that the two species are completely miscible for all crystalline structures in all proportions. The properties of the mixed crystals vary smoothly with the impurity content. No localized defect states associated with substitutional impurities are found either in the occupied or the virtual manifold. The relevance of the present results for simulation studies of germanium-containing silica glasses is discussed.

1. Introduction

The field of communications has experienced a revolution with the use of optical fibers which allow transmission of information at a much faster rate than conventional electrical guides, with many additional advantages, like chemical resistance to the environment, security of the transmission, and absence of electromagnetic contamination. One of the milestones in optical fibers technology, so far, has been the development, by Hill et al,[1] of a method for writing Bragg gratings in doped silica fibers, by means of a UV pattern. Bragg gratings avoid the need of photolithographic processes and are applied in a wide range of devices in the fields of telecommunications and stress sensors.

The microscopic mechanisms which allow the writing of gratings using UV radiation have been the subject of intense research, but a full understanding has not yet been achieved. It is clear, however, that germanium plays an important role as a dopant in silica fibers, and the photosensitivity is due to interaction of the UV radiation with germanium-related defects inside the silica structure.[2,3] Doping of silica with germanium is usually accomplished by mixing the two dioxides, SiO_2 and GeO_2, in different proportions, at the time of preparation of the glass. Often, some other dopants, like boron or sodium, are added and have been reported to also influence the photosensitivity of the glasses.[4] The dependence on so many different parameters makes the interpretation of the results difficult: theoretical calculations can be helpful in this respect, because they can isolate different aspects of the problem. Many kinds of defects have been studied theoretically in order to understand their structure and role in the optical activity. Most of them are based on the use of molecular cluster models;[5,6] recently, our group has addressed the question of how the energetic and optical properties of oxygen vacancies in silica are affected by the presence of nearby Ge impurities[7] using, instead, an embedding technique,[8] that is, the defective cluster is embedded in an otherwise perfect crystalline silica structure. However, a detailed investigation of how the presence of germanium in a relatively high concentration affects bulk properties of silica glasses remains, to our knowledge, undone.

Glasses represent a real challenge for quantum mechanical simulations. State of the art computational techniques can handle models containing a few hundreds of atoms, but this size may be insufficient to reproduce both the "infinite" network of chemical bonds and the lack of long-range order which are typical of those materials, apart from the fact that geometry optimization of such huge "molecules" may be a very heavy task. On the contrary, crystalline materials can be characterized much more effectively both from an experimental and a theoretical viewpoint. As concerns the latter aspect, exploitation of translational periodicity allows the problem to be effectively reduced to the size of the crystalline unit cell, and very accurate calculations are feasible at relatively low cost. Because the local bonding structure is common to most silica crystalline polymorphs and to the amorphous phases and is responsible for most of their properties, crystalline materials can be tentatively used as models to understand and analyze the changes in the bulk properties introduced by the presence of different proportions of impurity atoms. Furthermore, having at hand the solution (equilibrium configuration and ground-state electronic wave function) for a number of crystals with different germanium concentration and different geometric structures permits us to investigate a variety of local defective situations using appropriate embedding schemes.[8] Examples of this possibility will be presented in the last section.

In the present work, we have applied first principles quantum mechanical techniques to the study of periodic models of a

* To whom correspondence should be addressed.
† Unità INFM di Torino.
‡ Dipartimento di Chimica IFM.

10.1021/jp026931+ CCC: $25.00
Published on Web 03/12/2003

number of silica polymorphs containing different proportions of germanium as a substitutional species. To our knowledge no previous theoretical study of this kind exists, whereas a number of simulations of pure SiO_2 and GeO_2 structures have been performed, much more abundant in the former case because of its technological relevance. Reference is made in the following in particular to the studies by Nada et al.,[9] Silvi and co-workers,[10−14] and Ugliengo and co-workers,[15,16] who have adopted computational tools similar to those here employed.

Silicon dioxide displays an enormous variety of crystalline structures of comparable stability (zeolites are the best known example of this polymorphism), but only three of them have their germanium analogues: α-quartz, α-cristobalite, and stishovite; they contain 3, 4 and 2 XO_2 formula units per unit cell, respectively (here and in the following X is used to indicate the general Si or Ge atom). Stishovite is the stable phase of silica only at high pressures (>10 GPa): it has the rutile structure where coordination of silicon is six. The other two structures, as well as the enormous majority of the other silica polymorphs and silica glasses, are based on SiO_4 tetrahedra, and therefore, silicon atoms are 4-fold coordinated. The SiO_4 tetrahedral units display almost identical Si−O distances and O−Si−O angles in all of the different phases, but the Si−O−Si angle that determines the relative orientation between tetrahedra varies widely from one structure to the other. On the other hand, the total energy of the system does not depend strongly on the Si−O−Si angle. This justifies the existence of so many phases and the flexibility of silica glass and amorphous phases.

At variance with SiO_2, where the most stable low-pressure phase is α-quartz, GeO_2 crystallizes preferably as rutile. The two four-coordinated phases of GeO_2, α-quartz and α-cristobalite, differ considerably from the corresponding silica ones as far as X−O-X angles are concerned.[11,13]

Starting from these three basic structures, a number of "mixed crystals" can be created and characterized by substituting one or more atoms of Si with Ge. Because we have not used supercells, the number of structures of composition intermediate between pure silica and pure germanium oxide is two, three, and one for α-quartz, α-cristobalite, and rutile, respectively. In addition, we have considered the β-quartz structure which generates again two intermediate structures. The reason for treating also this phase, which is stable for silica only at high temperatures and is not known to exist for GeO_2, is that calculations are available from the literature concerning its equilibrium geometry and relative stability with respect to the other phases.[11,15]

From this study, information can be gained about the influence of the chemical composition on equilibrium geometry, relative stability, and electronic structure. It should allow us to predict whether strong distortions are created around substitutional atoms, whether impurities tend to aggregate in clusters, whether localized defect states are created in mixed crystals, and whether such features depend on the crystalline structure. Because all of the systems considered are very close in energy, the computational method adopted must satisfy strict requirements as concerns its reliability.

The techniques adopted are presented in section 2, and their validation is provided in section 3 with reference to the experimentally known facts about the pure phases. It is shown that the problem of the relative stability is a very delicate one, because balancing of the errors implicit in the different approximations adopted is far from obvious. However, this analysis has allowed us to select a basis set and a computational approach which is expected to give sensible results also for the mixed crystals. The results concerning these phases are presented and analyzed in section 4: it is shown that silicon and germanium are completely miscible for all crystalline structures in all proportions; the properties of the mixed crystals vary smoothly with the impurity content; no localized defect states associated with substitutional impurities are found either in the occupied or the virtual manifold. The relevance of the present results for simulation studies of germanium-containing silica glasses is discussed in section 5.

2. Models and Computational Details

A graphical representation of the four structures can be found in standard textbooks or on the Web.[17] We recall briefly some known facts about them. α-Quartz ($P3_21$ space group) is the most stable silica phase at room temperature; its density (ρ = 2.65 g/cm^3) is appreciably higher than that of vitreous silica (2.21 g/cm^3[18]). At a temperature of 847 K, it transforms into β-quartz ($P6_22$ space group; ρ = 2.53 g/cm^3). The β structure has beeen interpreted by Silvi et al.[11] as a resonance between two twin α-structures separated by a small energy barrier, and the fact that germanium dioxide does not display the β phase explained by those authors is due precisely to the much higher value of that barrier in this case (about four times larger than in silica). The stable phase of silica above 1750 K is α-cristobalite ($P4_12_1$ space group), whose density is 2.33 g/cm^3, the closest to that of silica glasses among the structures here considered. Finally, the rutile phase ($P4_2/mnm$ space group), which is the most stable polymorph at room temperature for germanium dioxide, is by far the densest one (for stishovite, ρ = 4.65 g/cm^3). In fact, the increase of the diffraction index in Bragg gratings following UV irradiation has been suggested by Sulimov[5] to be due to the formation of rutile-like structures in a vicinity of oxygen vacancies, resulting in a local densification of the glass. In the following, we will use the compact notation S(x) to describe the various systems investigated, where x is the molar fraction of germanium dioxide. For instance, $Q_\alpha(0)$ and $Q_\alpha(1/3)$ will denote two α-quartz structures where all the three atoms in the unit cell are Si or one of them has been substituted by Ge, respectively.

The sixteen systems here considered will then be indicated as follows:

$Q_\alpha(0)$, $Q_\alpha(1/3)$, $Q_\alpha(2/3)$, $Q_\alpha(1)$ (α-quartz structures)

$Q_\beta(0)$, $Q_\beta(1/3)$, $Q_\beta(2/3)$, $Q_\beta(1)$ (β-quartz structures)

C(0), C(1/4), C(1/2), C(3/4), C(1) (α-cristobalite structures)

R(0), R(1/2), R(1) (rutile structures)

The tool we have employed to simulate them is CRYSTAL,[19] a widely used computer program which solves the Schrödinger equation for periodic structures both in a Hartree−Fock (HF) and in a density functional theory (DFT) framework; it also allows the use of "hybrid-exchange" Hamiltonians as suggested by Becke.[20] The HF approximation has been used here routinely for the geometry optimizations, whereas energy estimates were obtained by using a DFT Hamiltonian with the gradient corrected exchange-correlation potential proposed by Perdew and Wang, usually indicated as PWGGA.[21] These choices are justified in the next section.

The geometry of the sixteen systems has been fully optimized. A beta-version of CRYSTAL has been used for this purpose which embodies the energy gradient with respect to internal

coordinates.[22] Such an option is badly needed in studies such as the present one; for instance, although the pure $Q_\alpha(0)$ and $Q_\alpha(1)$ phases require the optimization of 4 internal coordinates, these are 12 in the mixed $Q_\alpha(1/3)$ structure. Convergence in the structural relaxation has been considered achieved when the root-mean-square of gradients and displacements of ions has become smaller than 3.0×10^{-4} and 1.2×10^{-3} a.u., respectively, and their largest component smaller than 4.5×10^{-4} and 1.8×10^{-3} a.u., respectively. The lattice parameters of all of the compounds have been optimized manually: as we shall see, accounting for the changes in volume and shape of the cell is important.

CRYSTAL adopts a set of localized Gaussian-type functions centered in the atomic nuclei and with the angular features of standard atomic orbitals; each crystalline orbital is in turn described by a linear combination of such atomic orbitals. Apart from the choice of the Hamiltonian, selecting a suitable basis set is the most delicate methodological aspect in these kinds of calculations: in the next section, we discuss briefly how this selection has been done, with reference to past experience and to a specific analysis of the problems posed by the present study.

Let us add a few words about the other computational parameters. Special attention has been paid to obtain very good convergence in the total energy of the different compounds. This is required to evaluate accurately the relative stability of the polymorphs, because energy differences are very small. The self-consistent procedure is stopped when either of the following criteria is satisfied: the eigenvalues are converged up to 10^{-6} Hartree or the total energy per unit cell is converged up to 10^{-5} Hartree. The cutoff parameters ITOL 1−5 of CRYSTAL[23] for Coulomb and exchange integrals evaluation have been set to rather strict values (6,6,6,6,12) for all of the four-coordinated structures; to achieve the same quality of results, even stricter tolerances were adopted for the denser rutile structures (7,7,7,7,-14). Integration in reciprocal space is carried out using a commensurate and uniformly spaced grid.[24] The number of *k* points in the irreducible part of the Brillouin zone depends both on the shrinking factor adopted and on the symmetry of the system. For instance, 7 and 10 *k* points are required for $Q_\alpha(0)$ and $Q_\alpha(1/3)$, respectively; because denser *k*-point grids are necessary for hexa-coordinated compounds, as many as 105 sampling *k* points have been used for R(1/2) to obtain results of comparable accuracy.

3. Pure Phases: Choice of Basis Set and Hamiltonian

The basis set choice is a critical issue in this kind of calculations, because it determines the accuracy with which the calculated wave function and the derived quantities may approximate the exact solution. For instance, Civalleri et al.[15] have shown that the relative stability of silica polymorphs with tetrahedral Si coordination is correctly described only if polarization *d* functions are included in the Si and O sets. A main concern in our case has been to find a basis set able to describe consistently both tetra- and hexa-coordinated compounds. This problem has been already faced by Nada et al.[9] and Silvi et al.[12] Once more, the need for polarization *d* functions is outlined in both studies. The *d* orbitals in silicon play a fundamental role for the correct description of the partially covalent character of the Si−O bonding, influencing directly the Si−O equilibrium distance; those on oxygen are required to provide a correct description of the dependence of total energy on the Si−O−Si bond angle.[25] Our final choice has been based on the experience accumulated by the above-mentioned authors, who also used CRYSTAL for their studies. The present sets for the three atomic species are practically coincident with those they adopted except for minor adjustments needed for a balanced description of the different reference systems. Using the standard notation for Gaussian basis sets, the following choices have been adopted for the three atomic species: for silicon, a 6−211G* basis, with outer exponents $\alpha_{sp} = 0.25$ and $\alpha_d = 0.5$; for oxygen, a 6-311G* basis, with outer exponents $\alpha_{sp} = 0.905$, 0.265 and $\alpha_d = 0.4$; for germanium, a 9766(d)-31G* basis optimized by Zicovich-Wilson for the study of germanium containing zeolites,[26] with outer exponents $\alpha_{sp} = 0.248$ and $\alpha_d = 0.5582$. We think that this basis set is about the best possible presently for our problem, taking into account computational times and problems of quasi-linear-dependency which may occur when more diffuse functions are included.

TABLE 1: Calculated versus Experimental Values (when Available) of Some Geometrical Parameters for the Pure Phases Here Considered

		SiO_2		GeO_2	
phase		calcd	expt	calcd	expt
	a/Å	4.966	4.902[a]	5.026	4.984[e]
	c/Å	5.463	5.400	5.573	5.648
α-quartz	*V*/Å^3	116.676	112.375	121.921	
	XÔX/deg	145.95	142.4	132.93	130.3
	X−O/Å	1.615	1.613	1.721	
	a/Å	5.082	5.00[b]	5.290	
	c/Å	5.571	5.46	6.032	
β-quartz	*V*/Å^3	124.60	118.212	146.185	
	XÔX/deg	154.90		153.18	
	X−O/Å	1.612		1.708	
	a/Å	4.978	4.957[c]	5.097	
	c/Å	6.911	6.890	7.211	
cristobalite	*V*/Å^3	171.226	169.300	187.309	
	XÔX/deg	145.15	144.7	135.55	
	X−O/Å	1.612	1.609	1.728	
	a/Å	4.152	4.177[d]	4.304	4.398[f]
	c/Å	2.634	2.666	2.865	2.863
rutile	*V*/Å^3	45.392	46.515	53.073	55.377
	XÔX/deg	114.60	114.776	115.17	114.928
	X−O/Å	1.770	1.785	1.859	1.887

All geometry optimizations have been performed at the HF level of approximation. XÔX are the average angles and X−O the average bond distance. A deeper analysis of the OÔO angles is presented later in the text. Sources of experimental data are as follows: (a) Lager, G. A.; Jorgensen, J. D.; Rotella, F. J. *J. Appl. Phys.* **1988**, *21*, 182. (b)Wright, A. F.; Lehmann, M. S. *J. Solid State Chem.* **1981**, *36*, 371. (c) Pluth, J. J.; Smith, J. V.; Faber, J. J. *J. Appl. Phys.* **1985**, *57*, 1045. (d) Spackman, M. A.; Hill, R. J.; Gibbs, G. V. *Phys. Chem. Minerals* **1987**, *14*, 139. (e) Glinnemann, J.; King, H. E.; Schulz, H.; Hahn, T.; Laplaca, S. J.; Dacol, F. *Z. Kristallog.* **1992**, *198*. (f) Baur, W. H.; Khan, A. A. *Acta Cryst.* **1971**, *B27*, 2133.

The other and independent choice to be effected is the approximate scheme adopted for solving the Schrödinger equation. Among the one-electron Hamiltonians which are allowed by the CRYSTAL program, we considered the HF scheme and the DFT gradient corrected technique with the parametrization proposed by Perdew and Wang,[21] to be referred to in the following as PW−PW. In fact, all geometry optimizations here presented have been performed at the HF level of approximation for the sake of convenience: HF has been shown to provide accurate geometry predictions for silica[15] and GeO_2 polymorphs;[14] moreover, the algorithms for the evaluation of the energy gradients with respect to internal coordinates exhibit much less numerical noise with HF than with DFT Hamiltonians. The accuracy with which the geometry of the mixed structures is predicted can be assessed by comparing the results concerning the pure dioxides with the experimental data. Table 1 displays some selected structural parameters of the different polymorphs. The agreement with the experiment is fairly good,

TABLE 2: Energy Data (*i*) of Pure Phases and Difference Δ(*i*) with Respect to α-Quartz[a]

SiO_2	α-quartz	*β*-quartz	cristobalite	rutile
E_{HF}[b]	−438.8833	−438.8817	−438.8824	−438.8633
δE_{PW}[c]	−1.1966	−1.1979	−1.1986	−1.2341
δE_{BSSE}[d]	0.1265	0.1265	0.1265	0.1866
E_{PW-PW}[e]	−440.0764	−440.0735	−440.0741	−440.0721
Δ(a)		0.0016	0.0009	0.0199
Δ(a+b)		0.0003	−0.0011	−0.0175
Δ(a+b+c)		0.0036	0.0029	0.0440
Δ(d)		0.0029	0.0023	0.0043
GeO_2	α-quartz	*β*-quartz	cristobalite	rutile
E_{HF}[b]	−2225.1956	−2225.1921	−2225.1954	−2225.1960
δE_{PW}[c]	−2.3082	−2.3062	−2.3061	−2.3368
δE_{BSSE}[d]	0.1269	0.1269	0.1269	0.1888
E_{PW-PW}[e]	−2227.6611	−2227.6465	−2227.6562	−2227.6709
Δ(a)		0.0036	0.0002	−0.0004
Δ(a+b)		0.0036	0.0022	−0.0374
Δ(a+b+c)		0.0036	0.0029	0.0245
Δ(d)		0.0146	0.0049	−0.0098

[a] All energies are in Hartree per XO_2 unit (1 Hartree = 27.21 eV). [b] Total HF energies. [c] a posteriori DFT PW correlation correction. [d] estimate of BSSE. [e] DFT PW−PW energies. For details, see text.

with the largest discrepancy concerning the volume of the two quartz phases of SiO_2.

A satisfactory description of geometries does not guarantee that calculations reproduce correctly the other quantities, first of all ground state energies. This question has been addressed by several authors. Reference can here be made to the previously cited study of the relative stability of a number of tetrahedrally coordinated silica polymorphs,[15] as resulting from the use of HF, DFT, and hybrid-exchange techniques. The order of stabilities is practically independent of the method adopted, with α-quartz being in all cases the most stable structure. However, the various estimates of $\Delta_S E = E(S) - E(\alpha\text{-quartz})$ may vary by a factor of 2 depending on the technique adopted. The spread in stability between the various polymorphs is minimal with HF and maximal with local-density DFT estimates. HF energies may be approximately corrected by using appropriate a posteriori DFT functionals, which estimate the electron correlation energy on the basis of the density resulting from the self-consistent HF procedure: their use brings the HF results in line with the others. In the following, the a posteriori correction of HF energies has been estimated owing to the proposal by Perdew and Wang and is referred to as δE_{PW}.[21] Not only is this one of the best tested and most successful scheme of its kind, but it has been shown to perform satisfactorily for the tetrahedrally coordinated silica structures by Civalleri et al.[15] Following those authors, we shall use the HF−PW label to identify energies calculated using this compound scheme, whereas PW−PW will indicate "pure" PWGGA results.

The calculated HF energies for the eight pure structures are reported in the (a) rows of Table 2, and their difference with respect to α-quartz is reported in line Δ(a) of the same table. Qualitatively, the experimental order of stabilities is respected that is, in order of increasing total energy:

$$SiO_2:\ \alpha\text{-quartz} < (\beta\text{-quartz, cristobalite}) < \text{stishovite}$$

$$GeO_2:\ \text{rutile} < (\alpha\text{-quartz, cristobalite})$$

However, results are not satisfactory for the germanium structures, which are practically iso-energetic according to the HF estimates, whereas it is known that rutile is by far more stable than the others. This deficiency might be imputed to the HF neglect of electron correlation, which is expected to be more important for the dense rutile-type systems than for the other polymorphs. The δE_{PW} estimate of the correlation energy, reported in the (b) rows of the same table, shows in fact that the correction is appreciably larger for the hexa-coordinated structures. However, although it brings in the correct ordering for the germanium compounds, among silica polymorphs, stishovite becomes the most stable and cristobalite more stable than α-quartz [row Δ(a+b) of Table 2].

A possible explanation for this unsatisfactory result can be traced back to the so-called basis set superposition error (BSSE).[27] This error occurs when the basis functions centered in two different ions overlap and may reciprocally contribute to compensate for the intrinsic incompleteness of the basis set of the other ion, so artificially increasing the stability of the composite system with respect to the separate species. The higher coordination causes more basis functions to overlap with each other in the hexa- rather than in the tetracoordinated compounds, and therefore, we expect the BSSE to be larger for the former systems. To estimate this error, we have employed a counterpoise correction,[27] where the energetic effect of the "auxiliary" basis sets surrounding a given atom (A) is estimated by means of two calculations for the isolated atom: $\delta E_{BSSE,A} = E_{fullbasis,A} - E_{Abasis,A}$. It is important to realize that this correction may depend on the charge state of the ion in the crystal depending on its chemical environment. For instance, it is expected to be much higher if the silicon ion is in a 2+ than when it is in a 4+ charge state (practically no help comes to its description from basis functions outside in the latter case). To take account of this aspect of the problem, we have performed HF calculations for the various atomic species, by assigning to the atom different numbers of electrons; in each case, we evaluated the Mulliken net charge q_A on A and interpreted the resulting $\delta E_{BSSE,A}(q_A)$ as the error affecting the A ion with a net Mulliken charge q_A in the crystal. Using a linear interpolation of the correction with respect to the charge and summing over the three species in each case, we were so able to estimate the BSSE error for the different crystals. The results are reported in the (c) rows of Table 2, and their effect on the stability order is reported in rows Δ(a+b+c). Despite the relatively high quality of the basis sets adopted, it is seen that the counterpoise correction is very important. It is practically the same for the tetrahedrally coordinated polymorphs, but much higher for the rutile-type crystals, especially because of the contribution from the oxygen ions. This correction would make by far the rutile structures the least stable in all cases, at variance with experiment. On the other hand, it is known that the counterpoise contribution overcorrects the BSSE, and a more accurate treatment of this error is required which is deferred to a further study.

When the PW−PW technique is adopted instead, with no BSSE adjustment, the results are in qualitative agreement with the experiment, as shown in rows (d) and Δ(d) of Table 2. Specially noteworthy is the high instability of Ge-*β*-quartz with respect to Ge-α-quartz (much larger than in the silicon case), which justifies the nonexistence of that phase.[11] This agreement between theory and experiment is partly fortuitous, because other possible sources of error must be considered also in this case, in particular BSSE.

This discussion shows that the balancing of errors of various origin (the approximate treatment of exchange and correlation contributions to electron−electron interaction energy, basis set effects, etc.) is very delicate when systems are concerned which differ in geometry and electronic structure. Note incidentally

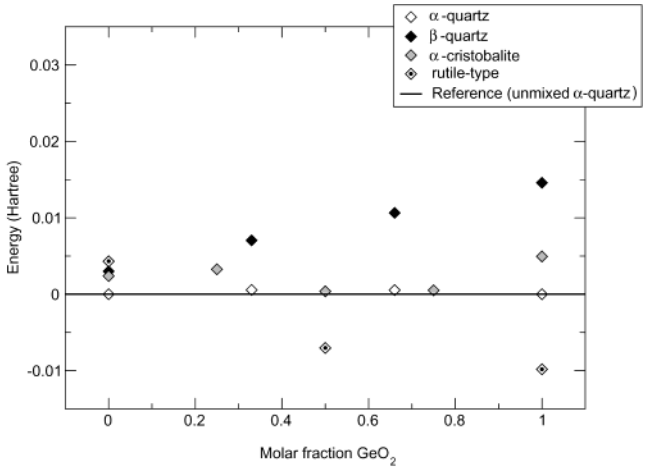

Figure 1. Stability of the different mixed systems S(x) with respect to a mixture of pure silicon and germanium α-quartz crystals with the same global composition, that is in a proportion $(1 - x)$:x. The data reported are the result of PW−PW calculations.

that $\Delta_S E$ values are in the order of a few kJ mol^{-1}, that is, 5 or 6 orders of magnitude less than $E(S)$. As is usual in these kinds of studies, we shall adopt in the following a rather empirical attitude and, on the basis of the above results, make reference to PW−PW calculations, without BSSE correction, to estimate the relative energies of the mixed crystals.

4. Results for the Mixed Crystals

An important question in the fabrication of the doped glasses is if the dopant will tend to cluster inside the host glass, therefore not forming a homogeneous mixture. To answer this question, we have compared the total energy per formula unit of the mixed crystal, $E[S(x)]$, with the energy of a mixture of the two pure α-quartz phases with the same global composition: $\Delta E_S(x) = E[S(x)] - \{(1 - x)\, E[Q_\alpha(0)] + x\, E[Q_\alpha(1)]\}$. These differences are reported in Figure 1, as resulting from PW−PW calculations. The energy of mixing is practically zero, as is shown by the fact that the $\Delta E_S(x)$ values are along a straight line for each S; if the entropic contribution is considered to take account of compositional disorder which exists in real systems, we may conclude that complete mixing is favored at all concentrations with respect to segregation of the impurities. Among the possible crystalline structures for the mixed systems, rutile is predicted to be the most stable starting from an x value of about 0.2, but this result is subject to all of the reservations put forward in the preceding section.

The same smooth dependence on the fraction of dopant is generally observed as concerns the geometrical parameters of the mixed systems. In particular, as expected, the cell volume increases almost linearly with x for all of the structures considered.

Part of the strain caused by the inclusion of germanium is released by means of a deformation of the network. The deformation implies a change in the structure in the XO_4 tetrahedral units that can be considered as the building blocks of the network in the tetracoordinated compounds. This is clear from Figure 2 which reports the range of O−Si−O angles (upper graph) and O−Ge−O angles (lower graph) as a function of the GeO_2 molar fraction for the three structures with tetrahedral coordination. Although the average value of those angles is practically constant and close to the ideal tetrahedral value (109.5°), the dispersion is considerably different from case to case: the fact that the range is systematically larger for

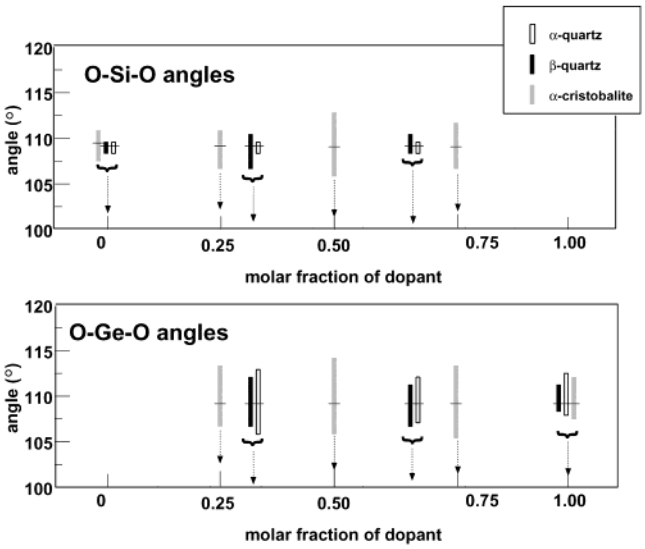

Figure 2. Graphs that analyze the distribution of O−Si−O angles (top plot) and O−Ge−O angles (bottom plot), for the various structures with tetrahedral coordination. Each bar represents the range, and the line across the bar represents the average value of the angles. White, black, and gray bars refer to compounds with α-quartz, β-quartz, and cristobalite structure, respectively. They are positioned along the x axis according to the molar fraction of GeO_2. All data refer to optimized HF geometries.

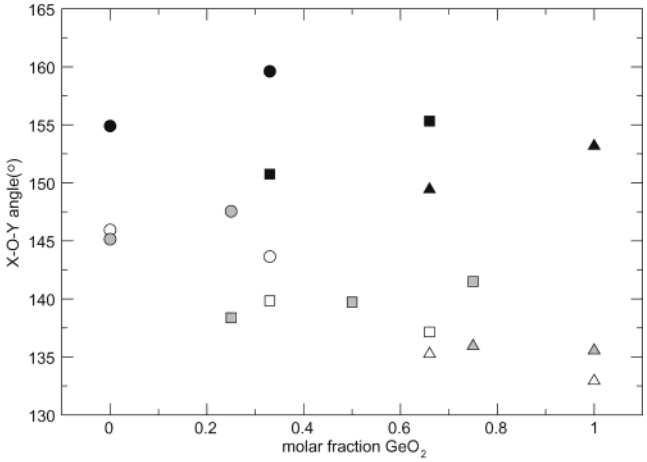

Figure 3. Value of the average X−O−Y angles. The circles represent Si−O−Si angles, the squares represent Si−O−Ge angles, and the triangles represent Ge−O−Ge angles. White, black, and gray symbols refer to compounds with α-quartz, β-quartz, and cristobalite structure, respectively. They are positioned along the x axis according to the molar fraction of GeO_2. All data refer to optimized HF geometries.

O−Ge−O shows that the GeO_4 tetrahedra are more flexible. As concerns SiO_4 tetrahedra, they become appreciably distorted only in C(1/2). The Si−O−Si, Ge−O−Si, and Ge−O−Ge angles present a similar evolution as silicon is being replaced by germanium, as it can be seen in Figure 3. In all systems, the Ge−O−Ge angles are always the narrowest, and the Si−O−Si angles are the widest, whereas the Si−O−Ge ones present values between the former ones. The changes in these angles are in any case more significant than the changes in the O−X-O angles (with X either Si or Ge), indicating that the structural flexibility of the silica network is due to its capacity to modify the relative orientation of the XO_4 structural units with respect to each other.

A remarkable difference between the pure silica and pure germanium dioxide phases can be seen in the analysis of the X−O-X angles already presented in Figure 3. Although in pure

TABLE 3: Mulliken Net Atomic Charges (q_A) and X−O Bond Populations (Q_{X-O}) as Obtained from the Hartree−Fock Calculations[a]

phase	x	q_O	q_{Si}	q_{Ge}	Q_{Si-O}	Q_{Ge-O}
	0	−1.199	2.398		0.241	
α-quartz	1/3	−1.271	2.408	2.810	0.242	0.162
	2/3	−1.344	2.423	2.820	0.243	0.162
	1	−1.416		2.832		0.162
	0	−1.195	2.390		0.240	
β-quartz	1/3	−1.261	2.379	2.805	0.242	0.162
	2/3	−1.332	2.366	2.812	0.244	0.163
	1	−1.400		2.799		0.164
	0	−1.198	2.396		0.242	
	1/4	−1.251	2.398	2.813	0.242	0.163
cristobalite	1/2	−1.309	2.404	2.809	0.245	0.165
	3/4	−1.355	2.400	2.813	0.246	0.163
	1	−1.406		2.812		0.165
	0	−1.406	2.813		0.105	
rutile	1/2	−1.477	2.804	3.104	0.120	0.069
	1	−1.499		2.998		0.091

[a] These quantities are defined as follows in terms of the one-electron density matrix P and of the overlap matrix S in the basis set of the atomic orbitals on atoms A, B, etc.: $q_A = Z_A - \sum_{\mu\in A}[PS]_{\mu\mu}$; $Q_{X-O} = \sum_{\mu\in A,\nu\in B}[PS]_{\mu\nu}$.

silica the difference between the Si−O−Si angle in α-quartz and that in β-quartz is almost 10°, in the case of pure germanium dioxide, the difference between the Ge−O−Ge angles of the α and β phases is almost 20°. Such a difference should increase the difficulty of the α to β transition in the case of pure germanium dioxide, as it is in fact the case because the β phase has not been detected.

Let us now discuss briefly the electronic structure of the sixteen systems.

A traditional tool for a preliminary characterization of the mode of binding of molecules and crystals[23] is the Mulliken population analysis, which subdivides the total electron charge into "atomic" and "bond" contributions. Despite the nonobservable character of these quantities (populations depend on the basis set adopted), interesting information can be obtained from data such as those reported in Table 3. From the net charges on oxygens, it is seen that ionicity increases systematically with increasing germanium content; in the case of four-coordinated structures, this is due simply to the fact that the Si−O bond has a stronger covalent character (larger bond population) than Ge−O. Rutile structures are much more ionic than the others, and their stability is essentially due to electrostatic interactions, as expected and as found in previous studies.[9]

We have also considered a more sophisticated topological analysis of the electron density distribution, as proposed by Bader,[29] using the TOPOND package.[30] We report here the most remarkable results of this analysis. The bond paths in all of the materials are close to the straight line that connects the two nuclei involved. The distance of oxygen from the critical point is almost independent from the type of material in the tetracoordinated structures (0.952 ± 0.005 Å along O−Si bonds and 0.911 ± 0.004 along O−Ge bonds) and is of course longer in the hexa-coordinated ones. The bonds have cylindrical symmetry, as indicated by the very low ellipticity, and their prevailingly ionic character may be inferred from the value of the Laplacian at the critical point ($\nabla^2(\mathbf{r}_c)$), which is positive in all cases, between 0.42 and 1.14 atomic units. However, quantitative interpretation of ($\nabla^2(\mathbf{r}_c)$) as a measure of the ionicity of the bond would bring us to conclusions in contradiction with the analysis just presented on the basis of the Mulliken analysis. In fact, ($\nabla^2(\mathbf{r}_c)$) is lower for the Ge−O bonds than for the Si−O

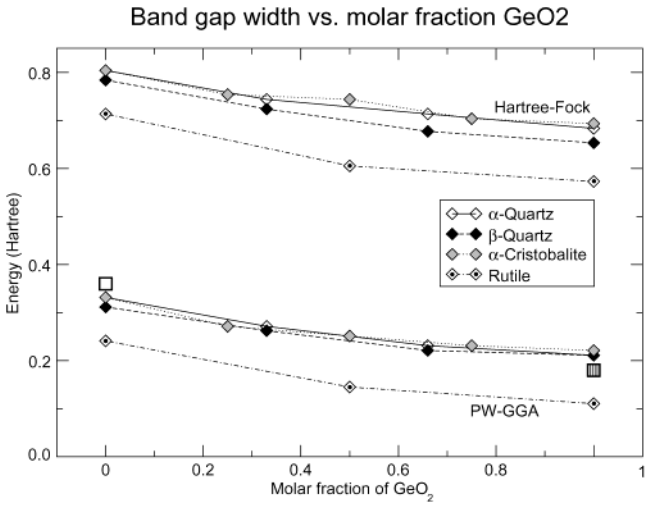

Figure 4. Dependence of the main gap on the molar fraction x of GeO_2 for the different structures, as resulting from HF (upper group of curves) or PW−PW (lower group) calculations. The experimental optical gap for pure silicon α-quartz is reported as a white square on the left; the estimated one for germanium rutile is reported as a dashed square on the right [Christie, D. M.; Chelikowsky, J. R. *Phys. Rev. B* **2000**, *62*, 14703].

ones and decreases considerably when passing from the tetra- to hexa-coordinated structures. The difficulty to characterize the Ge−O and, especially, the Si−O bond in terms of the information provided by ($\nabla^2(\mathbf{r}_c)$) only has already been emphasized in the deep study on this subject by Gibbs and co-workers.[31]

More physical insight about the electronic structure can be obtained from the composition and energy distribution of one-electron states. The complete miscibility of the two X species in all proportions entails as a consequence the close similarity of all band structures of a given S phase among themselves, irrespective of the value of x. To appreciate the differences in the electronic structure of the various compounds, it is convenient to make reference to quantities such as the band gap or the projected densities of states (PDOS) which may be compared to each other independently of the crystalline space group.

Figure 4 reports the values of all main gaps $E_{gap}[S(x)]$ calculated either with the HF or the PW−PW technique. As usual, HF exaggerates the distance between valence and conduction bands,[23] whereas PW−PW gives approximately the correct value. Qualitatively, the two computational approaches provide the same general description: $E_{gap}[S(x)]$ decreases smoothly with x, and its value is considerably smaller for the rutile-type systems. The main reason for the former effect is that antibonding Ge−O orbitals are lower in energy than those involving silicon; for the latter, that the rutile phases are much more ionic: the higher negative charge on oxygen makes all occupied bands associated to this species (in particular the top valence bands with prevailing p-O character) to come closer to the conduction bands. In addition, the p-O bands are wider in rutile because of the much higher density of the sublattice of oxygen ions in this case.[28]

All that is shown clearly in Figure 5, which reports PDOSs on oxygen and X atoms for a few selected pure and mixed structures and precisely: $Q_\alpha(0)$, $Q_\alpha(2/3)$, $Q_\alpha(1)$; R(0), R(1/2), R(1). This sampling is sufficient for the present analysis because PDOSs of the various tetracoordinated phases do not display noteworthy differences among themselves. The data in the figure are referring to HF calculations, but they are very similar to the PW−PW ones, except for a scaling in the energies near the Fermi level. With respect to silicon, Ge−PDOSs are character-

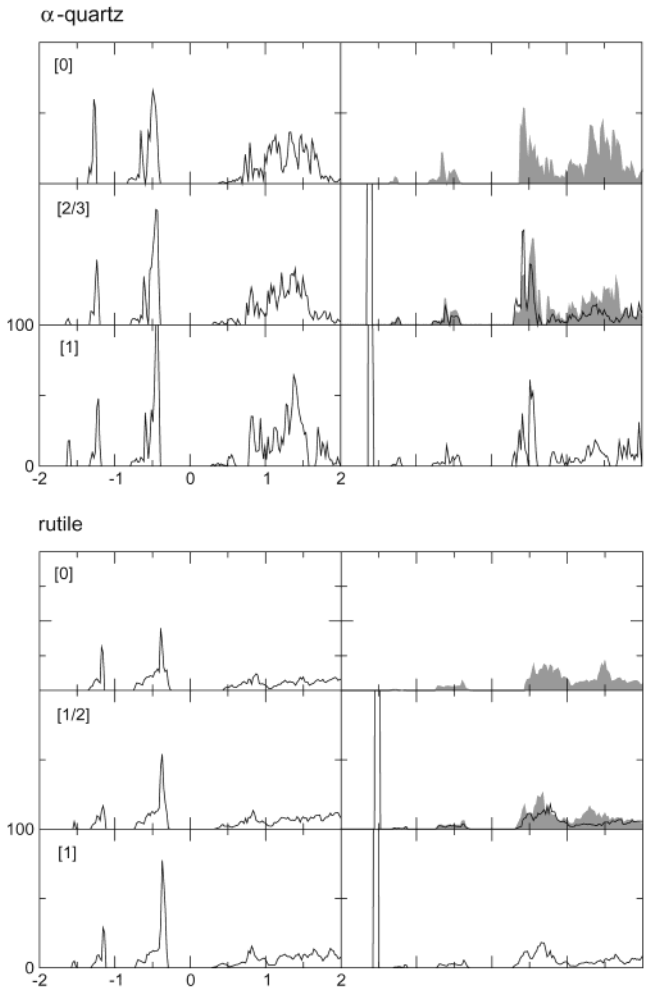

Figure 5. HF densities of one-electron states projected on oxygen (left panels) and X atoms (right panels) for some pure and mixed XO_2 structures. Projections are performed according to a Mulliken analysis. Each row corresponds to a system with a different concentration of Ge. The number in brackets indicates the molar fraction of Ge. In the right plots, gray areas and thin black lines correspond to Si and Ge projected densities, respectively. From top to bottom: $Q_\alpha(0)$, $Q_\alpha(2/3)$, $Q_\alpha(1)$; R(0), R(1/2), R(1). The scales are the same in all plots and precisely: on the horizontal axis, orbital energies from -2 to $+2$ Hartree; on the vertical axis, PDOS per atom per Hartree, from 0 to 100.

ized by the narrow and very high peak at about -1.6 Hartree, due to 3d states. For the rest, the two PDOSs are quite similar. In α-quartz, the presence of the directional X−O bonds is revealed by the high participation of X states in the *s*-O bands centered at about -1.3 Hartree and in the *p*-O bands in the region between -0.8 and -0.3 Hartree, and by the parallel oscillations of the PDOSs of O and X in these energy intervals. For rutile, both these features are less pronounced, that is, the PDOSs in these energy regions are less structured, and X contributions are less important. The differences between Si and Ge PDOSs are more remarkable in the virtual manifold of the pure phases: in particular, at the lower edge of the conduction bands, silicon exhibits a much higher DOS with respect to the other species. If we concentrate our attention on the mixed phases in the energy region between -1 and $+2$ Hartree which is the most significant for optical transitions, in no case a net distinction is found between the two X species as concerns the composition of the states. This seems to indicate that crystalline orbitals in this energy range have a fairly delocalized character and involve both species to about the same extent. One would have expected this to happen for the semicovalent tetrahedral compounds, but the fact that the same behavior is observed with rutile is somewhat surprising, given the rather net difference in the ionic character of the two species. The conclusion which can be derived from the present results is that in no case do substitional germanium impurities give rise to localized defect states either in the occupied or in the virtual manifold and to optical transitions of characteristic frequency. The presence of defects, such as oxygen vacancies or two-coordinated X species, could change the situation, giving origin to local structures where the distribution of vicinal germanium or silicon atoms makes a real difference.

5. Discussion and Conclusions

The photosensitivity of germanium-doped silica glasses has been interpreted generally as being due to defect-related processes; however, because high concentrations of dopant are often employed, knowledge about the overall changes in the electronic and geometric structure of the host material as a function of the impurity content is also required for a proper interpretation of such processes. The present study has treated this problem theoretically, by considering four different crystalline structures which contain SiO_2 and GeO_2 in various proportions. It has been shown that, for each phase, complete mixing of substitutional germanium takes place and that all properties, both geometrical and electronic, vary smoothly with the amount of doping. Among the different crystalline structures, rutile is predicted to be the most stable for impurity contents above 20%; this estimate is affected by considerable uncertainty because of the difficulty of calculating accurately energy differences in the range of a few kJ mol^{-1} which are parts in a million of the total electronic energy. With all such reservations, the present result may be significant for the understanding of Bragg grating formation upon UV irradiation. Although transition from a glassy to a crystalline phase is generally inhibited by large energy barriers, adsorption and re-emission of UV light in the presence of local defects and the consequent release of vibrational energy might result in the local formation of dense regions rich in quasi-rutile nanocrystals; according to the present study, such kinds of processes would be energetically favored by a relatively high concentration in germanium.

As concerns the possible modes of reorganization from tetra- to hexa-coordinated silica-like structures, reference can be made to a recent study by George and Catlow.[32] Using a semiclassical approach based on shell-model pair potentials between polarizable ions and on molecular dynamics techniques, they have simulated the transition between GeO_2 α-quartz and rutile. Interestingly, they have identified a saddle point for the activated transition (about 50 kJ mol^{-1}), where Ge ions exhibit either 4-fold or 6-fold coordination. First-principles calculations have been indeed employed to characterize transitions with change of coordination of pure Silica at high pressures; Silvi et al.[34] have characterized the transition from tetracoordinated cristobalite to hexa-coordinated stishovite phases, whereas Bingelli and Chelikowsky[33] have studied the transition from α-quartz to a rutile-like phase. Similar studies should be possible with the models that we have presented along this work. Also, more arbitrary reorganizations could be simulated by means of either supercell or embedded cluster models, in which the local structure can be rearranged freely, without any symmetry constraint.

The embedding techniques can also be utilized for defect studies, using the mixed systems characterized in the present study as host crystals. A variety of local situations can thus be

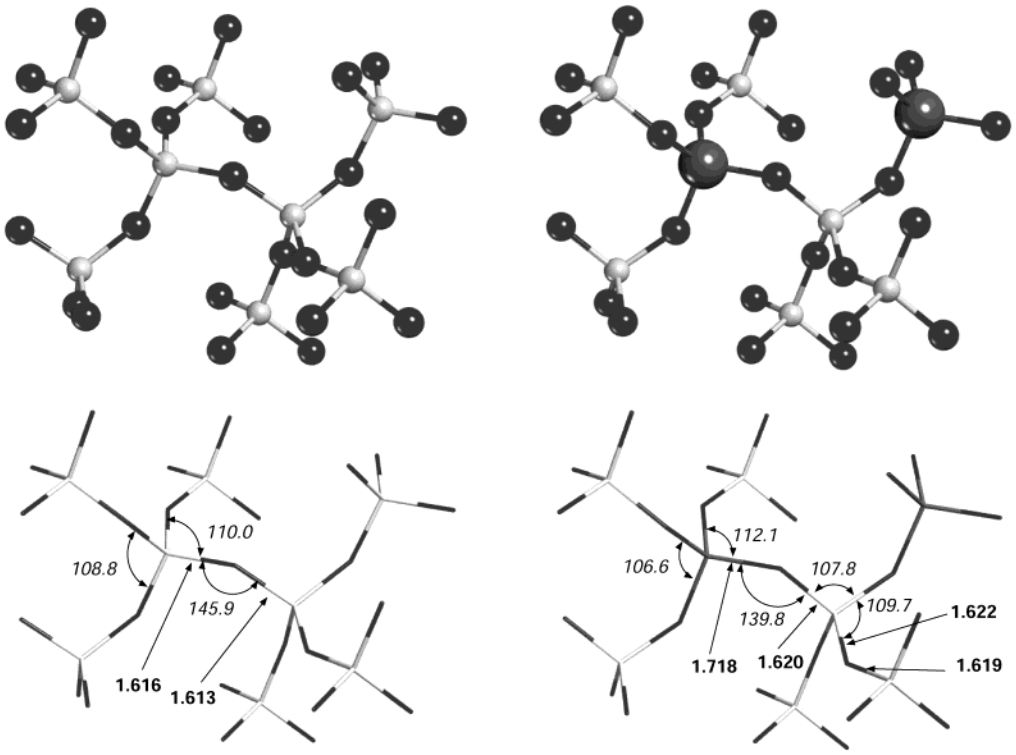

Figure 6. Schematic picture of clusters for a possible embedded-cluster study of an oxygen vacancy in Ge-doped silica glasses. Left: a 33 atom cluster cut out from pure Si-α-quartz; Right: one of the two possible clusters of the same kind, cut out from $Q_\alpha(1/3)$. Small white spheres represent silicon atoms, small gray spheres represent oxygen atoms, and big gray spheres represent germanium atoms. Some geometrical parameters, referring to the equilibrium configurations, are reported in the schemes below. The numbers in bold represent bond distances (in angstroms), and the numbers in italic represent angles (in degrees). Note that the higher symmetry of the nondoped cluster makes most of the distances and angles equivalent. See text for comments.

considered mimicking those found in real glasses and not existing in the pure phases. An example of such possibilities is reported in Figure 6. Two clusters are shown which could be used to simulate an oxygen vacancy in Ge doped silica glasses. On the left, the reference cluster is cut out from pure Si-α-quartz, and is of the kind used in our previous embedded cluster studies;[7] the defect-containing cluster is obtained by eliminating the central oxygen atom and substituting one or more silicon atoms with germanium. On the right, one of the two possible clusters of the same size and shape is shown, cut out from Q_α-(1/3). It is seen that the distribution of angles and distances is markedly different, and the presence of the impurity atoms near the vacancy does not require ad hoc substitutions.

Acknowledgment. The present work has been performed in the frame of the Research Training Network "ODUPE" (HPRN-CT-2000-00045) coordinated by B. Poumellec; F. Lopez-Gejo is the beneficiary of a one-year post-doc ODUPE bursary. The authors acknowledge the financial contribution of the European Commission through the Human Potential Program. Useful discussions with M. Ferraris, Y. Mencke, S. Casassa, B. Civalleri, C. Zicovich-Wilson, and P. Ugliengo are gratefully acknowledged.

References and Notes

(1) Hill, K. O.; Fujii, Y.; Johnson, D. C.; Kawasaki, B. S. *Appl. Phys. Lett.* **1978**, *32*, 647.
(2) Poumellec, B.; Kherbouche, F. *J. Phys. III France* **1996**, *6*, 1595.
(3) Skuja, L. *J. Non-Crys. Sol.* **1998**, *239*, 16.
(4) Chiesa, M.; Ferraris, M.; Giamello, E.; Milanese, M. *J. Non-Crys. Sol.* **2003**, in press.
(5) Sulimov, V. B.; Sokolov, V. O.; Dianov, E. M.; Poumellec, B. *Phys. Status Sol.(a)* **1996**, *158*, 155.
(6) Sulimov, V. B.; Sokolov, V. O.; Poumellec, B. *Phys. Stat. Sol. (b)* **1996**, *196*, 175. Uchino, T.; Takahashi, M.; Yoko, T. *Appl. Phys. Lett.* **2001**, *79*, 359. Pacchioni, G.; Mazzo, C. *Phys. Rev. B* **2000**, *62*, 5452.
(7) Busso, M.; Casassa, S.; Pisani, C.; Sulimov, V. B. *Model. Simul. Mater. Sci. Eng.* **2002**, *10*, 21.
(8) Pisani, C.; Corà, F.; Nada R.; Orlando R., *Comput. Phys. Commun.* **1994**, *82*, 139. Pisani, C.; Birkenheuer U. *Comput. Phys. Commun.* **1996**, *96*, 152.
(9) Nada, R.; Catlow, R. C.; Dovesi, R.; Pisani, C *Phys. Chem. Miner.* **1990**, *17*, 353.
(10) Dovesi, R.; Pisani, C.; Roetti, C.; Silvi, B *J. Chem. Phys.* **1987**, *86*, 6967.
(11) Silvi, B.; D'Arco, Ph.; Causà, M. *J. Chem. Phys.* **1990**, *93*, 7225.
(12) Silvi, B.; D'Arco, Ph.; Saunders, V. R.; Dovesi, R. *Phys. Chem. Miner.* **1991**, *17*, 674.
(13) Silvi, B.; Allavena, M.; Hannach, Y.; D'Arco, Ph. *J. Am. Cer. Soc.* **1992**, *75*, 1239.
(14) Jolly, L.-H.; Silvi, B.; D'Arco, Ph. *Eur. J. Miner.* **1994**, *6*, 7.
(15) Civalleri, B.; Zicovich-Wilson, C. M.; Ugliengo, P.; Saunders, V. R.; Dovesi, R. *Chem. Phys. Lett.* **1998**, *292*, 394.
(16) Catti, M.; Civalleri, B.; Ugliengo, P. *J. Phys. Chem. B* **2000**, *104*, 7259.
(17) http://cls-www.nrl.navy.mil/lattice/struk/sio2.html.
(18) Hobbs, L. W.; Yuan, X. In *Defects in SiO_2 and related dielectrics: Science and Technology*; Pacchioni, G., Skuja, L., Griscom, D. L., Eds.; Kluwer: Dordrecht 2000; p 37.
(19) Saunders, V. R.; Dovesi, R.; Roetti, C.; Causà, M.; Harrison, N. M.; Orlando, R.; Zicovich-Wilson, C. M. *Crystal98 User's Manual*; Università di Torino: Torino, Italy, 1998.
(20) Becke, A. D. *J. Chem. Phys.* **1993**, *98*, 5648.
(21) Perdew, J. P. In *Electronic Structure of solids*; Ziesche, P., Eschrig, H., Eds.; Akademie Verlag: Berlin, 1991; pp 11−20.
(22) Civalleri, B.; D'Arco, Ph.; Orlando, R.; Saunders, V. R.; Dovesi, R. *Chem. Phys. Lett.* **2001**, *348*, 131.
(23) Pisani, C.; Dovesi, R.; Roetti, C. *Hartree−Fock Ab Initio Treatment of Crystalline Systems*; Lecture Notes in Chemistry Vol. 48; Springer: Berlin, 1988.
(24) Monkhorst, H. J. *Phys. Rev B* **1969**, *20*, 1504.
(25) Bär, M. R.; Sauer, J. *Chem. Phys. Lett.* **1994**, *226*, 405.
(26) Zicovich-Wilson, C. M.; Corma, A. *J. Phys. Chem. B* **2000**, *104*, 4134.

(27) Boys, S. F.; Bernardi, F. *Mol. Phys.* **1970**, *19*, 553. Davidson, E. R.; Feller, D. *Chem. Rev.* **1986**, *86*, 681.
(28) Lichanot, A.; Gelizé, M.; Larrieu, C.; Pisani, C. *J. Phys. Chem. Sol.* **1991**, *52*, 1155. Dovesi, R.; Roetti, C.; Freyria-Fava, C.; Aprà, R.; Saunders, V. R.; Harrison, N. M. *Philos. Trans. R. Soc. London A* **1992**, *341*, 203.
(29) Bader, R. F. W. *Atoms in Molecules − A Quantum Theory*; University of Oxford Press: Oxford, 1990.
(30) Gatti, C. *TOPOND96 User's Manual*; CNR-CSRSRC: Milano, Italy, 1997.
(31) Gibbs, G. V.; Rosso, K. M.; Teter, D. M.; Boisen, M. B.; Bukowinski, M. S. T. *J. Mol. Struct.* **1999**, *13−25*, 485.
(32) George, A. R.; Catlow, C. R. A. *J. Solid State Chem.* **1996**, *127*, 137.
(33) Binggeli, N.; Chelikowsky, J. R.; *Nature* **1991**, *353*, 344.
(34) Silvi, B.; Jolly, L.-H.; D'Arco, Ph.; *J. Mol. Struct. (THEOCHEM)* **1992**, *260*, 1.